

1  
2  
3  
4  
5  
6  
7  
8  
9  
10  
11  
12  
13  
14  
15  
16  
17  
18  
19  
20  
21  
22  
23  
24

*Distinct microbial communities alter litter decomposition rates in a fertilized coastal plain wetland*

Megan E. Koceja<sup>1</sup>, Regina B. Bledsoe<sup>1</sup>, Carol Goodwillie<sup>1</sup>, and Ariane L. Peralta<sup>1,†</sup>

<sup>1</sup>Department of Biology, East Carolina University, Howell Science Complex, Mail Stop 551,  
Greenville, NC 27858, USA

†Corresponding author: telephone: +1 252.328.2712, e-mail: [peralaa@ecu.edu](mailto:peralaa@ecu.edu)

Author contributions: MEK, RBB, CG, and ALP conceived and designed the research; MEK, RBB, and ALP collected and analyzed the data; MEK and ALP wrote the manuscript; all authors performed field work and edited the manuscript.

25 **ABSTRACT**

26 Human activities have led to increased deposition of nitrogen (N) and phosphorus (P) into soils.  
27 Nutrient enrichment of soils is known to increase plant biomass and rates of microbial litter  
28 decomposition. However, interacting effects of hydrologic position and associated changes to soil  
29 moisture can constrain microbial activity and lead to unexpected nutrient feedbacks on microbial  
30 community structure-function relationships. Examining how feedbacks of nutrient enrichment on  
31 decomposition rates is essential for predicting microbial contributions to carbon (C) cycling as  
32 atmospheric deposition of nutrients persists. This study explores how long-term nutrient addition  
33 and contrasting litter chemical quality influence soil bacterial community structure and function.  
34 We hypothesize that long-term nutrient enrichment of low fertility soils alters bacterial community  
35 structure and leads to higher rates of litter decomposition with decreasing C:N ratio of litter; but  
36 low nutrient and dry conditions limit constrain microbial decomposition of high C:N ratio litter.  
37 We leverage a long-term fertilization experiment to test how nutrient enrichment and hydrologic  
38 manipulation (due to ditches) affects decomposition and soil bacterial community structure in a  
39 nutrient poor coastal plain wetland. We conducted a litter bag experiment and characterized litter-  
40 associated and bulk soil microbiomes using 16S rRNA bacterial sequencing and quantified litter  
41 mass losses and soil physicochemical properties. Results revealed that distinct bacterial  
42 communities were involved in decomposing higher C:N ratio litter more quickly in fertilized  
43 compared to unfertilized especially under drier soil conditions, while decomposition rates of green  
44 tea litter (lower C:N ratio) were similar between fertilized and unfertilized plots. Bacterial  
45 community structure in part explained litter decomposition rates, and long-term fertilization and  
46 drier hydrologic status affected bacterial diversity and increased decomposition rates. However,  
47 community composition associated with high C:N litter was similar in wetter plots with available

48 nitrate detected, regardless of fertilization treatment. This study provides insight into long-term  
49 fertilization effects on soil bacterial diversity and composition, decomposition, and the increased  
50 potential for soil C loss as nutrient enrichment and hydrology interact to affect historically low  
51 nutrient ecosystems.

52

53 Keywords: biodiversity-ecosystem function; carbon cycling; decomposition; microbiomes; tea bag  
54 index; wetlands.

55

## 56 INTRODUCTION

57 Humans modify their landscapes through fossil fuel burning, deforestation, and intense  
58 agricultural activity (Vitousek et al. 2010, Fowler et al. 2013). These anthropogenic disturbances  
59 have led to increased atmospheric deposition of nitrogen (N) and phosphorus (P), and can be  
60 particularly disruptive to historically nutrient-limited ecosystems (Guignard et al. 2017). This  
61 increased nutrient deposition can cause a fertilization effect on plant-microbial interactions which  
62 results in increased biomass and shifts in community structure (Cherif and Loreau 2009, Leff et  
63 al. 2015, Harpole et al. 2016). This fertilization effect can increase plant biomass C, which fuels  
64 heterotrophic microbial growth and leads to increased respiration of CO<sub>2</sub> (Hoosbeek et al. 2004,  
65 Kuzyakov 2010). The extent to which nutrient enrichment predicts decomposition rates is also  
66 determined by the interaction of soil microorganisms with the plant inputs and the abiotic soil  
67 environment. While human alteration of the environment and its effect on C storage and release is  
68 relatively well-documented in terrestrial ecosystems, the mechanisms governing the interactive  
69 effects of nutrient enrichment on plant-soil-microbial relationships at terrestrial-aquatic interfaces  
70 are relatively understudied. The availability of terminal electron acceptors in hydrologically

71 dynamic ecosystems are known to shape the resident microbial community and to control  
72 biogeochemical functions (Bernhardt et al. 2017). This makes it challenging to predict microbial  
73 responses to environmental change in ecosystem models.

74 Changes in the nutrient stoichiometry of both plants and surrounding soils are expected to  
75 affect microbial community composition and function, leading to changes in elemental cycling.  
76 Prior studies have shown that long-term nutrient addition enhances grassland plant biomass and  
77 increases C inputs into soils (e.g., Harpole et al. 2016). These additional plant inputs also increase  
78 CO<sub>2</sub> outputs via microbial respiration (Hoosbeek et al. 2004, Lange et al. 2015). If microbes are  
79 not limited by N and P, the increase in plant-derived organic C inputs are more quickly metabolized  
80 and soil CO<sub>2</sub> fluxes increase (Peralta and Wander 2008, Cotrufo et al. 2013, Castellano et al. 2015).  
81 Plant biomass could also vary in C:N or C:P ratios, which could also cause changes in microbial  
82 nutrient use and respiration rates. Thus, it is important to understand how changes in available  
83 nutrients within plant litter alter microbial communities and CO<sub>2</sub> respiration rates as surrounding  
84 environmental conditions also shift (Hoosbeek et al. 2004, Lange et al. 2015).

85 Nuanced interactions between litter chemical quality, abiotic environment, and resident  
86 microbial composition can manifest in similar decomposition patterns (i.e., increased rates due to  
87 increased nutrient availability). However, the degree to which microbial structure contributes to  
88 the magnitude of litter mass loss is challenging to pinpoint since interactions among abiotic  
89 (temperature, nutrient availability, moisture) and biotic (community structure) factors determine  
90 decomposition rates (Kuzyakov and Blagodatskaya 2015, Meier et al. 2017, Deveau et al. 2018).  
91 In this study, we examine the extent that litter-associated microbiomes are unique depending on  
92 historical nutrient enrichment and how this community composition contributes to decomposition  
93 of litter of varying chemical quality (i.e., C:N ratio).

94           The nutrient availability in upland conditions makes priming (using standing litter  
95 nutrients) more pronounced as aerobic respiration is more energetically favored. In this study, we  
96 measured the extent that microbial community change (due to nutrient enrichment) contributes to  
97 enhanced decomposition using a model litter comparison. The Tea Bag Index (TBI) compares the  
98 decomposition rates of two different plant litters, green and rooibos Lipton™ tea bags (Keuskamp  
99 et al. 2013). Green tea has a measured mean C:N ratio of 12.229 while rooibos tea is measured to  
100 have a much higher mean C:N ratio of 42.870. We used the TBI protocol to examine how long-  
101 term fertilization affects decomposition rates in a nutrient-limited coastal plain wetland ecosystem.  
102 We also characterized the bacterial communities (using targeted amplicon sequencing of the V4  
103 region of the 16S rRNA gene) associated with the litter decomposition of two differing litter types  
104 (green and rooibos teas) occurring in wetland soils exposed to fertilization or not. The extent that  
105 community composition matters to decomposition rate depends on biotic and abiotic factors. In  
106 this study, litter type, nutrient enrichment and hydrologic status resulted in distinct bacterial  
107 communities.

108

## 109 **MATERIALS AND METHODS**

110

### 111 *Experimental design of a long-term ecological experiment*

112           Initiated in 2003, a long-term ecological experiment started at East Carolina University's  
113 West Research Campus (WRC) (35.6298N, -77.4836W) examines the effects of mowing and  
114 fertilization on coastal plain wetland plant and microbial communities. This study site is classified  
115 as a jurisdictional wetland, and the plant community has been described as a mosaic of wet pine  
116 flatwood habitat, pine savanna, and hardwood communities (Chester 2004). The soils were

117 characterized as fine, kaolinitic, thermic Typic Paleaquults (Coxville series), fine-loamy, siliceous,  
118 semiactive, thermic Aeric Paleaquults (Lynchburg series), and fine-loamy, siliceous, subactive,  
119 thermic Aquic Paleudults (Goldsboro series). These soils are moderately to poorly drained ultisols  
120 (USDA NRCS 2019). The annual mean temperature is 16.4 °C and annual precipitation is 126 cm  
121 (U.S. Climate Data 2019). Fertilization and mowing treatments are replicated on eight 20×30 m  
122 blocks in a full factorial design, and the N-P-K 10-10-10 pellet fertilizer is applied 3× per year  
123 (February, June, and October) for a total annual supplementation of 45.4 kg/ha for each nutrient.  
124 Plots are mowed by bush-hog annually to simulate fire disturbance (Goodwillie et al. In Review).  
125 Within each plot, annual soil and plant sampling takes place at three randomly-placed quadrats  
126 (Fig. 1). The plant community in plots that are mowed is dominated by perennial forbs in two  
127 major genera of the Asteraceae—*Eupatorium* and *Solidago*—and graminoid species. The relative  
128 abundance of major grass species differs between mowed and fertilized plots, with switchcane  
129 (*Arundinaria tecta*) most dominant in fertilized plots and broomsedge (*Andropogon virginicus*)  
130 found almost exclusively in unfertilized plots. Sedges (e.g., *Rhychospora* and *Carex* spp.) and  
131 species of *Juncus* are common in (wet) plots away from, but not in (dry) plots adjacent to the  
132 drainage ditch. This hydrologic gradient is caused by a roadside drainage ditch such that four  
133 blocks near the ditch are drier and four blocks away from the ditch are wetter (Goodwillie et al. In  
134 Review). In 2018, volumetric soil moisture content (measured by capacitance), was >2 times  
135 wetter in blocks away from the ditch compared to blocks adjacent to the ditch. However, this  
136 hydrologic gradient has not yet been characterized by modeling flow according to water levels  
137 over time. The ditch was not intentionally manipulated as part of our experimental design, but it  
138 contributes an important ecological variable to the study (Goodwillie et al. In Review). For this  
139 study, tea litter decomposition experiments were focused in the mowed plots only.

140

141 *Soil sampling*

142 We collected composite soil samples from all mowed/unfertilized and mowed/fertilized  
143 plots, which represented two soil cores (12 cm depth, 3.1 cm diameter) adjacent to each of three  
144 permanently installed 1 m<sup>2</sup> quadrats where plant community data are annually collected. Each  
145 composite bulk soil sample was passed through a 4 mm sieve and homogenized before further  
146 analysis. This bulk soil sampling occurred on November 14, 2019, about three months after the tea  
147 litter bags were collected from the field.

148

149 *Soil physico-chemical analyses*

150 We measured gravimetric soil moisture by weighing 20-30 g of field-moist soil, drying at  
151 105 °C overnight, and then re-weighing. We calculated percent moisture as difference between  
152 field-moist and dried soils divided by the oven-dried soil weight. In addition, we measured pH of  
153 oven-dried soil by mixing a 1:1 soil:water solution and using a pH probe (Genemate-Bioexpress;  
154 Kaysville, Utah; USA). We measured total soil organic carbon and total nitrogen on finely ground  
155 dried soil using an elemental analyzer (2400 CHNS Analyzer; Perkin Elmer; Waltham,  
156 Massachusetts, USA) at the Environmental and Agricultural Testing Service laboratory  
157 (Department of Crop and Soil Sciences at North Carolina State University). Extractable inorganic  
158 N for each soil sample was measured on approximately 5 g of field moist soil. We added 45 ml of  
159 2 M KCl to soil, shook the sample for about 1 hour, and gravity filtered. Total phosphate (PO<sub>4</sub><sup>3-</sup>)  
160 was extracted by combining 0.1 g dried soil (ground and passed through a 500 µm sieve) with 0.5  
161 ml of 50% w/v Mg(NO<sub>3</sub>) and ashing for 2 hours at 550 °C. Samples were hydrated with 10 mL of  
162 1 M HCl, shaken for 16 hours at 250 RPM, and the filtered (22 µm filter). Water extractable PO<sub>4</sub><sup>3-</sup>

163 was determined by combining 1 g dried soil (ground and passed through a 500  $\mu\text{m}$  sieve) with  
164 deionized water, shaken for 1 hour, and filtered (22  $\mu\text{m}$  filter). Ammonium ( $\text{NH}_4^+$ ), nitrate ( $\text{NO}_3^-$ ),  
165 and  $\text{PO}_4^{3-}$  ions in soil extracts were colorimetrically measured using a SmartChem 200 auto  
166 analyzer (Unity Scientific Milford, Massachusetts, USA) at the East Carolina University  
167 Environmental Research Laboratory.

168

### 169 *Field experimental methods*

170 The field protocol for this experiment was adapted from the Tea Bag Index Protocol  
171 (Keuskamp et al. 2013) and applied within the eight-replicate fertilized and unfertilized plots of  
172 the WRC. The experimental setup involved three bags of Lipton™ green tea and three bags of  
173 Lipton™ rooibos tea per replicate plot (3 bags  $\times$  8 blocks  $\times$  2 treatment plots = 48 bags per each  
174 tea bag type). In each treatment plot, we prepared six holes about 20 cm apart and 8 cm deep using  
175 a hand trowel. We weighed green and rooibos tea bags and buried them in separate holes. Soil was  
176 lightly packed around the tea bags, while keeping the labels visible above the soil. Tea bags were  
177 recovered after 111 days (May 21–September 09, 2018) using hand trowels to loosen soil adjacent  
178 to tea bag locations. Two of three green tea bags at each replicate plot were measured for mass  
179 loss. The third green tea bag was placed into a sterile Whirl-pak bag and stored at  $-20\text{ }^\circ\text{C}$  for tea-  
180 associated bacterial community analysis. The rooibos tea was processed following the same  
181 procedure. Upon returning to the lab, the tea bags for decomposition analysis were separated from  
182 adhered soil particles, placed into individual aluminum weighing dishes, and oven-dried at  $70\text{ }^\circ\text{C}$   
183 for 48 hours. To quantify mass loss, the tea bags were reweighed following drying and compared  
184 to their initial weight prior to soil incubation.

185



186 *Soil and tea-associated bacterial 16S rRNA sequencing*

187       Following freezing, tea litter was removed from tea bags, and DNA was extracted from  
188 samples using the Qiagen DNeasy PowerSoil kit. We also extracted DNA from soils using the  
189 Qiagen DNeasy PowerSoil Kit. For each unfertilized or fertilized treatment, DNA was extracted  
190 from green tea (15 total), rooibos tea (14 total), and bulk soil samples (16 total). Three litter  
191 samples could not be located and were not retrieved from the field. Following extraction, sample  
192 DNA was used as template in PCR reactions with a bacterial 515F/806RB barcoded primer set  
193 originally developed by the Earth Microbiome Project to target the V4-V5 region of the bacterial  
194 16S subunit of the rRNA gene (Apprill et al., 2015; Caporaso et al., 2012; Parada et al., 2016). For  
195 each sample, three 50  $\mu$ L PCR libraries were prepared by combining 35.75  $\mu$ L molecular grade  
196 water, 5  $\mu$ L Amplitaq Gold 360 10x buffer, 5  $\mu$ L MgCl<sub>2</sub> (25 mM), 1  $\mu$ L dNTPs (40mM total,  
197 10mM each), 0.25  $\mu$ L Amplitaq Gold polymerase, 1  $\mu$ L 515 forward barcoded primer (10  $\mu$ M), 1  
198  $\mu$ L 806 reverse primer (10  $\mu$ M), and 1  $\mu$ L DNA template (10 ng/ $\mu$ L). Thermocycler conditions for  
199 PCR reactions were as follows: initial denaturation (94 °C, 3 minutes); 30 cycles of 94 °C for 45  
200 seconds, 50 °C for 30 seconds, 72 °C for 90 seconds; final elongation (72 °C, 10 minutes).  
201 Triplicate PCR reactions were combined for each sample and cleaned according to the Axygen®  
202 AxyPrep Magnetic Bead Purification Kits protocol (Corning Life Sciences). Following cleaning,  
203 PCR product were quantified using Quant-iT dsDNA BR (broad-range) assay (Thermo Scientific,  
204 Waltham, MA, USA). Libraries were pooled in equimolar concentration of 5 ng/ $\mu$ L after being  
205 diluted to a concentration of 10 ng/ $\mu$ L. The Indiana University Center for Genomics and  
206 Bioinformatics sequenced the pooled libraries using the Illumina MiSeq platform using paired-end  
207 reads (Illumina Reagent Kit v2, 500 reaction kit).

208           Following sequencing, we processed raw sequences using a standard mothur pipeline  
209 (v1.40.1) (Schloss et al. 2009, Kozich et al. 2013). Contigs were assembled from paired end reads  
210 and quality trimmed using a moving average quality score (minimum score of 35 bp). Sequences  
211 were aligned to the SILVA rRNA gene database (v.128) (Quast et al. 2013) and chimeric  
212 sequences were removed using the VSEARCH algorithm (Rognes et al. 2016). Formation of  
213 operational taxonomic units (OTUs) involved dividing sequences based on taxonomic class and  
214 then binned into OTUs with a 97% sequence similarity level. OTUs were classified using the  
215 SILVA database (Yilmaz et al. 2014, Glöckner et al. 2017).

216

### 217 *Statistical analyses*

218           All statistical calculations were completed in the R environment (R v3.6.3, R Core  
219 Development Team 2020). Decomposition was measured through mass loss of buried tea bags.  
220 Initial and final tea bag weights were used to determine percent of loss. We ran a linear mixed  
221 effects model with ‘source’, ‘treatment’, and ‘ditch proximity’ as fixed effects and ‘block’ as a  
222 random effect using the lmer() function in the lmerTest package (Kuznetsova et al. 2017). For the  
223 mass loss response variable, a linear mixed model was fit by REML and produced type II analysis  
224 of variances tables (ANOVA) tables based on the Kenward-Roger's denominator degrees of  
225 freedom method using the lmerModLmerTest() function. Calculations of decomposition rate ( $k$ )  
226 and stabilization factor ( $S$ ) for each tea bag were accomplished according to formulas found within  
227 the TBI protocol. Decomposition rate,  $k$ , is a parameter representing short-term dynamics of new  
228 input decomposition, while stabilization factor,  $S$ , is a parameter characterizing long-term carbon  
229 storage. These values were used to draw comparisons between  $k$  and  $S$  values found within the  
230 WRC wetland ecosystem to those of global ecosystems submitted to the Tea Bag Index protocol

231 (Keuskamp et al. 2013). Outcomes of these calculations were plotted on a graph, and locations of  
232 groupings were compared to those of the larger multi-ecosystem index (Keuskamp et al. 2013).

233 For the bulk soil factors measured and the computed diversity (OTU richness, Shannon  
234 Diversity, Simpson's Evenness) metrics for soil and tea litter associated bacterial communities, we  
235 ran a series of linear mixed models. We ran linear mixed effects models with 'source', 'treatment'  
236 and 'ditch' as fixed effects and 'block' as a random effect and fitted by the REML criterion using  
237 the lmer() function in the lmerTest package (Kuznetsova et al. 2017). Statistical inferences for  
238 fixed effects were calculated from type II ANOVA tables and the Kenward-Roger's degrees of  
239 freedom method using the anova() function.

240 To visualize the community responses to fertilization and litter type, we used principal  
241 coordinates analysis (PCoA) of bacterial community composition based on the Bray-Curtis  
242 dissimilarity. We used a permutational multivariate analysis of variance (PERMANOVA) to  
243 examine among-treatment differences in bacterial communities. We also include a comparison of  
244 the bulk soil and tea litter associated bacterial communities (PERMANOVA, PCoA ordination)  
245 but focused on the specific tea litter associated microbiome patterns. To identify which bacterial  
246 species were most representative of each litter type, we ran an indicator species analysis. For the  
247 indicator species analysis, we only included bacterial taxa with a relative abundance greater than  
248 0.05 when summed across all plots. We performed PERMANOVA using the adonis() function in  
249 the vegan package (Oksanen et al. 2017) and the indval() function in the indicpecies package  
250 (Caceres and Jansen 2016).

251 To examine structure-function relationships between the tea-associated bacterial  
252 community and the mass loss of the tea litter, we ran a linear regression to measure the relationship  
253 between mass loss as a function of bacterial diversity (mass loss ~ OTU richness + Shannon

254 Diversity + Simpson's Evenness). In addition, we conducted a distance-based partial least squares  
255 regression (dbplsr) measure how much variation in mass loss of litter (function) was explained by  
256 the tea-associated bacterial community composition (structure) (mass loss ~ bacterial community).  
257 We used the Bray-Curtis dissimilarity matrix and the generalized cross-validation estimate of the  
258 prediction error ('gcv' method). We performed a distance-based partial least squares regression  
259 analysis using the dbplsr() function in the dbstats and pls packages (Boj Del Val et al. 2007, Boj  
260 et al. 2017, Mevik et al. 2019).

261

## 262 **RESULTS**

263 Long-term fertilization strongly influenced abiotic and biotic factors within this nutrient-  
264 limited wetland environment. Both fertilization and ditch effects influenced soil pH, soil C:N ratio,  
265 extractable nitrate concentrations, and water extractable phosphorus (Table S1A, Table S2B). A  
266 subset of soil factors was distinct between fertilized and unfertilized soils in the mowed plots. Total  
267 and water extractable phosphorus concentrations, extractable nitrate concentrations, soil C and N  
268 content, moisture, and pH were higher in fertilized compared to unfertilized soils (Table S1B). In  
269 addition, soil moisture, C:N ratio, and water extractable phosphorus were higher in wetter soils  
270 away from the ditch compared to drier soils adjacent to the ditch (Table S1C). Finally, nitrate  
271 concentrations were detectable only in wetter soils away from the ditch with higher concentrations  
272 in fertilized soils compared to unfertilized soils while nitrate was below detection limits in all soils  
273 near the ditch (Table S1A). These differences in fertilized compared to unfertilized soils and soil  
274 moisture due to ditch proximity related to litter decomposition rates and altered bacterial  
275 community structure.

276 To examine how litter type and nutrient addition influenced decomposition rates, we  
277 measured mass loss of green (low C:N litter) and rooibos (high C:N litter) tea bags. Following an  
278 111-day incubation, there was a significant litter type (source)  $\times$  fertilization treatment interaction  
279 ( $P=0.05$ ) (Fig. 2, Table S2). The mass loss of green tea litter was  $\sim 24\%$  higher than the overall  
280 mass loss of rooibos tea litter (Fig. 2, Table S2), averaged across fertilized and unfertilized soils.  
281 Both fertilization and proximity to drainage ditch also increased the rate of mass loss (Fig. 2, Table  
282 S2). Across all tea types and drainage ditch proximities, fertilized soils showed an average mass  
283 loss of  $\sim 7.5\%$  more than that of unfertilized soils. Tea bags buried in closer proximity to the  
284 drainage ditch had  $\sim 6\%$  more mass loss averaged across all litter and treatment types.

285 We also compared the decomposition rates ( $k$ ) and stabilization factors ( $S$ ) from the long-  
286 term fertilization experiment to a broader context of ecosystems (Keuskamp et al., 2013). The most  
287 variable  $S$  and  $k$  values were measured in the wetter, fertilized plots (Fig. 3). The unfertilized  
288 compared to fertilized samples were generally higher along the stabilization factor ( $S$ ) axis.  
289 Samples that were buried in the wetter, fertilized plots clustered along the higher end of the  
290 stabilization factor ( $S$ ), while litter buried in the drier plots (fertilized and unfertilized) had lower  
291 estimated stabilization factor ( $S$ ) (Fig. 3). Upon comparison with other ecosystems, a large number  
292 of fertilized treatment samples grouped near the grassland-ambient ecosystem in Iceland and the  
293 forest ecosystem in the Netherlands (Keuskamp et al. 2013). However, the unfertilized treatment  
294 samples grouped near the peat-disturbed and peat-undisturbed ecosystems of Iceland and the peat  
295 ecosystem of the Netherlands (Keuskamp et al. 2013). Within this coastal plain wetland system,  
296 long-term nutrient enrichment shifted decomposition rates that were representative of grassland  
297 and forested ecosystems (fertilized plots) or peatlands (unfertilized plots) (Fig. 3).

298 Fertilization effects on soil physicochemical properties and decomposition rates were  
299 related to shifts in bulk soil and litter-associated bacterial communities. Fertilization effect, tea  
300 type, and proximity to ditch (i.e., wetter vs. drier plots) influenced bacterial diversity in various  
301 ways. Specifically, tea type ( $R^2=0.130$ ,  $P=0.001$ ) influenced bacterial community composition the  
302 most, while the interaction of tea type and proximity to ditch affected bacterial community patterns  
303 to a lesser degree ( $R^2=0.060$ ,  $P=0.002$ ) (Fig. 4, Table S3) (see circle vs triangle). The proximity to  
304 ditch (proxy for hydrology) also altered bacterial community composition ( $R^2=0.110$ ,  $P=0.001$ )  
305 (Fig. 4, Table S3) (see opened vs filled). Within tea type, fertilization treatment influenced  
306 bacterial community composition ( $R^2=0.070$ ,  $P=0.003$ ) (Fig. 4, Table S3) (see green vs gray). For  
307 the drier, ditched plots, bacterial communities associated with high C:N ratio litter (rooibos)  
308 overlapped despite fertilization treatment, while bacterial communities were distinct between  
309 fertilization treatments in the wetter plots (Fig. 4). When the bulk soil and tea-associated bacterial  
310 communities were analyzed together, bulk soil or tea most strongly influenced bacterial  
311 community composition (source:  $R^2=0.490$ ,  $P=0.001$ ) (Fig. S1, Table S4). In addition to these  
312 observed patterns, OTU diversity was generally higher in fertilized compared to unfertilized plots,  
313 especially in the drier plots associated with the drainage ditch (Fig. 5, Table S5). Specifically, OTU  
314 richness values were highest in bulk soil compared to tea types (Fig. 5A, Table S5A), and Shannon  
315 diversity values were highest in bulk soil compared to tea type in fertilized plots (Fig. 5B, Table  
316 S5B). Lastly, bacterial evenness was similar across fertilization treatment, source type, and  
317 proximity to ditch (Fig. 5C, Table S5C).

318 To further examine bacterial associations with litter decomposition, we used indicator  
319 species analysis to identify a subset of bacterial taxa that represented each of the bulk soil or tea  
320 associated microbiomes. The unclassified OTU within the class Spartobacteria and another OTU

321 within the order Acidobacteria Gp1 represented the unfertilized bulk soil bacterial community,  
322 while an unclassified OTU within the order Solirubrobacterales represented bulk soils in the  
323 fertilized, dry plots. In wetter plots, an unclassified OTU within the order Rhodospirillales  
324 represented unfertilized plots while unclassified taxa within the orders Acidobacteria Gp1, Gp2,  
325 and Gp6 signified fertilized bulk soils (Tables S6, S7). In addition, the unclassified OTU within  
326 the Acidobacteria Gp3 and *Dongia* spp. represented the green tea-associated (low C:N litter)  
327 bacterial communities in the unfertilized, dry plots while *Conexibacter* spp. were represented in  
328 the fertilized, dry plots. In the wetter plots, *Phenylobacterium* spp. represented green tea-  
329 associated bacterial communities in unfertilized plots and *Legionella* spp. in fertilized plots. The  
330 OTUs *Acidisoma* spp. in unfertilized plots and *Dyella* spp. in fertilized characterized rooibos tea  
331 associated bacterial communities in the dry plots. Lastly, the OTU *Lacibacterium* spp. represented  
332 mowed plots, while *Dokdonella* spp. and an unclassified OTU within the genus *Microbacteriaceae*  
333 represented rooibos tea associated communities in the wet plots (Tables S6, S7).

334 When examined together, the link between bacterial community structure and  
335 decomposition function was relatively weak. No relationship between litter mass loss and bacterial  
336 diversity was detected ( $R^2_{adj} = -0.038$ ,  $P = 0.574$ ). However, when the total bacterial community  
337 was considered, the tea-associated bacterial community accounted for ~64 % of the variation in  
338 litter mass loss (dbplsr, Component 1  $R^2_{adj} = 63.56$ , Component 2  $R^2_{adj} = 87.09$ , Component 3  $R^2_{adj}$   
339 = 93.96) (Table 1).

340

## 341 **DISCUSSION**

342 Litter composition, fertilization, and ditch effects on soil moisture influenced bacterial  
343 community structure-function relationships in unexpected ways. In this study, increases in litter

344 mass loss were greater in fertilized compared to unfertilized soils, especially in drier versus wetter  
345 plots. Surprisingly, distinct microbial communities associated with different litter chemical  
346 qualities. Litter mass loss following the field incubation indicates that similar bacterial  
347 communities are capable of decomposing higher C:N ratio litter (rooibos tea) more quickly in  
348 fertilized compared to unfertilized plots, particularly in drier compared to wetter plots. However,  
349 lower C:N ratio litter (green tea) decomposition rates were similar among fertilized and  
350 unfertilized plots, although slightly higher in drier compared to wetter plots but were represented  
351 by distinct bacterial communities. As expected, the low C:N ratio litter provides a N source to  
352 microbes regardless of external soil nutrient conditions, whereas the high C:N ratio litter is reliant  
353 on N from the fertilized soil in order to support increased rates of litter decomposition (Duddigan  
354 et al. 2020). These results suggest that shifts in microbial community composition are partly due  
355 to differences in litter chemical quality and nitrate availability in soils.

356         The comparative results from the TBI-based decomposition experiment indicate that the  
357 tea litter bags buried in the unfertilized treatment had decomposition rates ( $k$ ) and C stabilization  
358 factor ( $S$ ) values similar to that of peatland ecosystems (Keuskamp et al. 2013). Lower  
359 decomposition rates occurred in unfertilized plots (i.e., the ambient state of this nutrient-poor  
360 habitat). When looking specifically at high C:N ratio litter, less mass was lost to decomposition.  
361 This provides some evidence that C storage potential within these plots resembles that of peatlands  
362 (Hill et al. 2018). Wetland ecosystems that are disconnected and isolated from pulses of nutrients  
363 due to natural processes or agricultural or urban runoff are more commonly nutrient limited by N  
364 and P (Vitousek et al. 2010). The plant species that are adapted to these low-nutrient ecosystems  
365 can maintain positive population growth and contribute to organic C additions to soils. Further,  
366 flooded environments, such as wetlands, are also known to support anaerobic microbial processes,



367 which result in slower rates of decomposition (Collins et al. 2015). Taken together, low nutrient  
368 environments can be sites of high plant biodiversity leading to organic C inputs and balanced with  
369 slower decomposition rates, which contribute to long-term C storage in soils (Hooper et al. 2005,  
370 Kleber et al. 2011). These results reflect the coastal plain wetland environment in this study, which  
371 offers some evidence that wetland environments store a disproportionate amount of C compared  
372 to other ecosystems (Sutfin et al. 2016, Nahlik and Fennessy 2016). However, this C storage  
373 capacity can be disrupted by nutrient enrichment. The fertilized plots, however, had  $k$  and  $S$  values  
374 that grouped closer towards grassland and forest ecosystems (Riggs et al. 2015), which have lower  
375 C storage potential because more available nutrients and oxic environments support aerobic  
376 respiration and higher decomposition rates. Results from this study provide support that nutrient  
377 enrichment can have a lasting influence on plant-soil-microbe interactions that affect C storage  
378 potential of wetland ecosystems (Lambers et al. 2009, Allison et al. 2014, Hartman et al. 2017).

379       Patterns in bacterial community composition (i.e., beta diversity) but not the combined  
380 OTU richness, Shannon diversity, Simpson's evenness diversity metrics, significantly explained  
381 decomposition rates. Further, litter composition followed by the fertilization and ditch effects  
382 determined bacterial community composition. A trend of higher decomposition rates was  
383 associated with high bacterial diversity, especially in the fertilized compared to unfertilized plots.  
384 Higher diversity has been associated with higher decomposition rates across different ecosystems  
385 (Lange et al. 2015, Trivedi et al. 2016). Shifts in plant and microbial communities can fuel  
386 decomposition rates and ultimately C losses from historically low nutrient ecosystems that  
387 experience atmospheric nutrient deposition (Sardans and Peñuelas 2012, Wieder et al. 2015).

388       When bulk and tea-associated microbiomes were considered together, the bulk soil  
389 bacterial communities were very distinct from the tea-associated bacterial communities. Within

390 the bulk soil, bacterial communities were distinct across fertilized and unfertilized dry plots, and  
391 indicator taxa were phylogenetically distinct at the phylum level (Proteobacteria vs.  
392 Acidobacteria). While results revealed similarity in bulk soil bacterial composition in the fertilized  
393 and unfertilized wet plots, the indicator taxa also represented distinct phyla (unfertilized:  
394 Verrucomicrobia + Acidobacteria, fertilized: Actinobacteria). In contrast, the indicator taxa for  
395 tea-associated bacterial communities that overlapped in composition were similar at the phylum  
396 level. Specifically, similar bacterial assemblages of rooibos tea-associated (high C:N litter)  
397 microbiomes in the fertilized and unfertilized, dry plots were associated with Proteobacteria (Table  
398 S6, unfertilized: *Lacibacterium spp.*, fertilized: *Dokdonella spp.*). Indicator bacterial taxa  
399 representing high C:N ratio litter-associated microbiomes in fertilized, dry plots were *Dokdonella*  
400 *spp.* (Proteobacteria phylum) and unclassified Microbacteriaceae (Actinobacteria phylum). The  
401 genus *Dokdonella* has been involved in heterotrophic denitrification (Figueroa-González et al.  
402 2016, Palma et al. 2018), while members of the family Microbacteriaceae have been  
403 predominantly found in terrestrial and aquatic ecosystems with putative functions related to plant  
404 pathogenicity (Glöckner et al. 2000, Young 2008, Lory 2014). Indicator taxa within the order  
405 Alphaproteobacteria represented the similar bacterial communities of the high C:N litter-  
406 associated microbiomes in unfertilized (indicator OTU *Acidisoma spp.*), wet plots and low C:N  
407 litter-associated microbiomes in unfertilized, dry plots (indicator OTU *Phenylobacterium spp.*). In  
408 addition, the community similarity between low C:N litter-associated microbiomes in unfertilized,  
409 wet plots and high C:N litter-associated microbiomes in fertilized, wet plots were represented by  
410 taxa within different Proteobacterial classes. Specifically, *Dongia spp.* (within  
411 Alphaproteobacteria class) and *Dyella spp.* (within Gammaproteobacteria class) are similar in at  
412 least some life history traits. Representative isolates were cultured from soils (*Dyella*) and wetland

413 sediments (*Dongia*) and were found to be aerobic, Gram-negative, and motile (Xie and Yokota  
414 2005, Baik et al. 2013). Further, these assemblages also overlapped with green tea-associated  
415 microbiomes in the fertilized, dry plots, which were represented by *Legionella spp.* (within class  
416 Gammaproteobacteria). Legionellae are found in aquatic and other moist environments with their  
417 free-living protozoan hosts (Barker and Brown 1994). In the wetland soil environment, they can  
418 persist but are unlikely existing under optimal conditions.

419         The interaction between source (litter type) and fertilization treatment influenced mass loss  
420 of litter but hydrologic setting and soil nitrate altered litter-associated microbiomes to varying  
421 degrees. The ditch-derived hydrologic differences at this wetland resulted in different structure-  
422 function relationships for high C:N ratio litter-associated microbiomes only. Under the relatively  
423 dry plots (i.e., near drainage ditch), microbiomes associated with high C:N ratio litter were similar,  
424 but mass loss of litter was higher in fertilized compared to unfertilized plots. In all other instances,  
425 distinct, fertilized microbiomes were associated with higher decomposition rates compared to  
426 unfertilized plots. In the case that community structure is the same and decomposition rates  
427 increase, this pattern provides some evidence of more severe N limitation in drier compared to  
428 wetter plots, where soil nitrate concentrations are below detection limits (Table S1B). This result  
429 was only observed under high C:N ratio litter context since the low C:N litter provided much  
430 needed N to litter-associated microbes. While soil ammonium levels are similar in this case, it is  
431 possible that N mineralization is occurring without limitation, but nitrification processes could be  
432 slowed due to low soil pH, resulting in differences in extractable soil nitrate but not ammonium  
433 concentrations (Hinckley et al. 2019).

434         In this study, nutrient enrichment and hydrologic status resulted in distinct bacterial  
435 communities associated with litter and bulk soils. Drier conditions and nutrient enrichment

436 increased decomposition rates until N limitation constrains microbial community structure. This  
437 study provided the opportunity to compare the extent that community composition matters to  
438 decomposition rate – using model litter. In these nutrient poor wetland soils undergoing nutrient  
439 enrichment, the fertilization increased bacterial diversity the potential for increased C losses  
440 through decomposition is observed and is expected to increase as wetlands are drained and  
441 fertilized.

442

#### 443 **ACKNOWLEDGMENTS**

444 We thank Allison Fisk, Emma Richards, Tom Vogel, John Stiller, Suelen Tullio, and Adam Gold  
445 for laboratory and field assistance. We thank John Gill and the East Carolina University grounds  
446 crew for their tireless efforts in maintaining the long-term ecological experiment. This work was  
447 supported by the East Carolina University Undergraduate Research and Creative Activity Award  
448 to MEK and the National Science Foundation (GRFP to RBB, DEB 1845845 to ALP). All code  
449 and data used in this study can be found in a public GitHub repository  
450 ([https://github.com/PeraltaLab/WRC18\\_RhizoTeaDecomp](https://github.com/PeraltaLab/WRC18_RhizoTeaDecomp)) and the NCBI SRA (BioProject).

451

452

453

454

455

456

457

458

459 **LITERATURE CITED**

- 460 Allison, S. D., S. S. Chacon, and D. P. German. 2014. Substrate concentration constraints on  
461 microbial decomposition. *Soil Biology and Biochemistry* 79:43–49.
- 462 Apprill A, McNally S, Parsons R, and Weber L. 2015. Minor revision to V4 region SSU rRNA  
463 806R gene primer greatly increases detection of SAR11 bacterioplankton. *Aquatic  
464 Microbial Ecology* 75:129–137.
- 465 Baik, K. S., Y. M. Hwang, J.-S. Choi, J. Kwon, and C. N. Seong. 2013. *Dongia rigui* sp. nov.,  
466 isolated from freshwater of a large wetland in Korea. *Antonie van Leeuwenhoek*  
467 104:1143–1150.
- 468 Barker, J., and M. R. W. Brown. 1994. Trojan Horses of the microbial world: protozoa and the  
469 survival of bacterial pathogens in the environment. *Microbiology* 140:1253–1259.
- 470 Bernhardt, E. S., J. R. Blaszczak, C. D. Ficken, M. L. Fork, K. E. Kaiser, and E. C. Seybold.  
471 2017. Control Points in Ecosystems: Moving Beyond the Hot Spot Hot Moment Concept.  
472 *Ecosystems* 20:665–682.
- 473 Boj Del Val, E., M. M. C. Bielsa, and J. Fortiana. 2007. Selection of Predictors in Distance-  
474 Based Regression. *Communications in Statistics - Simulation and Computation* 36:87–  
475 98.
- 476 Boj, E., A. Caballe, P. Delicado, and J. Fortiana. 2017. dbstats: Distance-Based Statistics.
- 477 Caceres, M. D., and F. Jansen. 2016. indicpecies: Relationship Between Species and Groups of  
478 Sites.
- 479 Caporaso, J. G., C. L. Lauber, W. A. Walters, D. Berg-Lyons, J. Huntley, N. Fierer, S. M.  
480 Owens, J. Betley, L. Fraser, M. Bauer, N. Gormley, J. A. Gilbert, G. Smith, and R.

- 481 Knight. 2012. Ultra-high-throughput microbial community analysis on the Illumina  
482 HiSeq and MiSeq platforms. *The ISME Journal* 6:1621–1624.
- 483 Castellano, M. J., K. E. Mueller, D. C. Olk, J. E. Sawyer, and J. Six. 2015. Integrating plant litter  
484 quality, soil organic matter stabilization, and the carbon saturation concept. *Global*  
485 *Change Biology* 21:3200–3209.
- 486 Cherif, M., and M. Loreau. 2009. When microbes and consumers determine the limiting nutrient  
487 of autotrophs: a theoretical analysis. *Proceedings of the Royal Society B: Biological*  
488 *Sciences* 276:487–497.
- 489 Chester, R.E. 2004. Floristic assessment of a wet mineral flat at the East Carolina University  
490 West Research Campus and investigation of influential, human-mediated factors on the  
491 plant community. Master's Thesis, East Carolina University, Greenville, NC.
- 492 Collins, D. P., W. C. Conway, C. D. Mason, and J. W. Gunnels. 2015. Decomposition of three  
493 common moist-soil managed wetland plant species. *Journal of Fish and Wildlife*  
494 *Management* 6:102–111.
- 495 Cotrufo, M. F., M. D. Wallenstein, C. M. Boot, K. Deneff, and E. Paul. 2013. The Microbial  
496 Efficiency-Matrix Stabilization (MEMS) framework integrates plant litter decomposition  
497 with soil organic matter stabilization: do labile plant inputs form stable soil organic  
498 matter? *Global Change Biology* 19:988–995.
- 499 Deveau, A., G. Bonito, J. Uehling, M. Paoletti, M. Becker, S. Bindschedler, S. Hacquard, V.  
500 Hervé, J. Labbé, O. A. Lastovetsky, S. Mieszkin, L. J. Millet, B. Vajna, P. Junier, P.  
501 Bonfante, B. P. Krom, S. Olsson, J. D. van Elsas, and L. Y. Wick. 2018. Bacterial–fungal  
502 interactions: ecology, mechanisms and challenges. *FEMS Microbiology Reviews*  
503 42:335–352.

- 504 Duddigan, S., L. J. Shaw, P. D. Alexander, and C. D. Collins. 2020. Chemical underpinning of  
505 the Tea Bag Index: an examination of the decomposition of tea leaves. Research Article,  
506 Hindawi. <https://www.hindawi.com/journals/aess/2020/6085180/>.
- 507 Figueroa-González, I., G. Quijano, I. Laguna, R. Muñoz, and P. A. García-Encina. 2016. A  
508 fundamental study on biological removal of N<sub>2</sub>O in the presence of oxygen.  
509 Chemosphere 158:9–16.
- 510 Fowler, D., M. Coyle, U. Skiba, M. A. Sutton, J. N. Cape, S. Reis, L. J. Sheppard, A. Jenkins, B.  
511 Grizzetti, J. N. Galloway, P. Vitousek, A. Leach, A. F. Bouwman, K. Butterbach-Bahl, F.  
512 Dentener, D. Stevenson, M. Amann, and M. Voss. 2013. The global nitrogen cycle in the  
513 twenty-first century. Phil. Trans. R. Soc. B 368:20130164.
- 514 Glöckner, F. O., P. Yilmaz, C. Quast, J. Gerken, A. Beccati, A. Ciuprina, G. Bruns, P. Yarza, J.  
515 Peplies, R. Westram, and W. Ludwig. 2017. 25 years of serving the community with  
516 ribosomal RNA gene reference databases and tools. Journal of Biotechnology 261:169–  
517 176.
- 518 Glöckner, F. O., E. Zaichikov, N. Belkova, L. Denissova, J. Pernthaler, A. Pernthaler, and R.  
519 Amann. 2000. Comparative 16S rRNA analysis of lake bacterioplankton reveals globally  
520 distributed phylogenetic clusters including an abundant group of Actinobacteria. Applied  
521 and Environmental Microbiology 66:5053–5065.
- 522 Goodwillie, C., M. W. McCoy, and A. L. Peralta. In Review. Long-term fertilization, mowing,  
523 and ditch drainage interact in wetland plant communities.
- 524 Guignard, M. S., A. R. Leitch, C. Acquisti, C. Eizaguirre, J. J. Elser, D. O. Hessen, P. D.  
525 Jeyasingh, M. Neiman, A. E. Richardson, P. S. Soltis, D. E. Soltis, C. J. Stevens, M.  
526 Trimmer, L. J. Weider, G. Woodward, and I. J. Leitch. 2017. Impacts of Nitrogen and

527 Phosphorus: From Genomes to Natural Ecosystems and Agriculture. *Frontiers in Ecology*  
528 *and Evolution* 5.

529 Harpole, W. S., L. L. Sullivan, E. M. Lind, J. Firn, P. B. Adler, E. T. Borer, J. Chase, P. A. Fay,  
530 Y. Hautier, H. Hillebrand, A. S. MacDougall, E. W. Seabloom, R. Williams, J. D.  
531 Bakker, M. W. Cadotte, E. J. Chaneton, C. Chu, E. E. Cleland, C. D'Antonio, K. F.  
532 Davies, D. S. Gruner, N. Hagenah, K. Kirkman, J. M. H. Knops, K. J. L. Pierre, R. L.  
533 McCulley, J. L. Moore, J. W. Morgan, S. M. Prober, A. C. Risch, M. Schuetz, C. J.  
534 Stevens, and P. D. Wragg. 2016. Addition of multiple limiting resources reduces  
535 grassland diversity. *Nature* 537:93–96.

536 Hartman, W. H., R. Ye, W. R. Horwath, and S. G. Tringe. 2017. A genomic perspective on  
537 stoichiometric regulation of soil carbon cycling. *The ISME Journal* 11:2652–2665.

538 Hill, B. H., C. M. Elonen, A. T. Herlihy, T. M. Jicha, and G. Serenbetz. 2018. Microbial  
539 coenzyme stoichiometry, nutrient limitation, and organic matter decomposition in  
540 wetlands of the conterminous United States. *Wetlands Ecology and Management* 26:425–  
541 439.

542 Hinckley, B. R., J. R. Etheridge, and A. L. Peralta. 2019. Wetland Conditions Differentially  
543 Influence Nitrogen Processing within Waterfowl Impoundments. *Wetlands*.

544 Hooper, D. U., F. S. Chapin, J. J. Ewel, A. Hector, P. Inchausti, S. Lavorel, J. H. Lawton, D. M.  
545 Lodge, M. Loreau, S. Naeem, B. Schmid, H. Setälä, A. J. Symstad, J. Vandermeer, and  
546 D. A. Wardle. 2005. Effects of biodiversity on ecosystem functioning: a consensus of  
547 current knowledge. *Ecological Monographs* 75:3–35.

548 Hoosbeek, M. R., M. Lukac, D. van Dam, D. L. Godbold, E. J. Velthorst, F. A. Biondi, A.  
549 Peressotti, M. F. Cotrufo, P. de Angelis, and G. Scarascia-Mugnozza. 2004. More new



550 carbon in the mineral soil of a poplar plantation under Free Air Carbon Enrichment  
551 (POPFACE): Cause of increased priming effect? *Global Biogeochemical Cycles* 18.  
552 Keuskamp, J. A., B. J. Dingemans, T. Lehtinen, J. M. Sarneel, and M. M. Hefting. 2013. Tea  
553 Bag Index: a novel approach to collect uniform decomposition data across ecosystems.  
554 *Methods in Ecology and Evolution* 4:1070–1075.  
555 Kleber, M., P. S. Nico, A. Plante, T. Filley, M. Kramer, C. Swanston, and P. Sollins. 2011. Old  
556 and stable soil organic matter is not necessarily chemically recalcitrant: implications for  
557 modeling concepts and temperature sensitivity. *Global Change Biology* 17:1097–1107.  
558 Kozich, J. J., S. L. Westcott, N. T. Baxter, S. K. Highlander, and P. D. Schloss. 2013.  
559 Development of a dual-index sequencing strategy and curation pipeline for analyzing  
560 amplicon sequence data on the MiSeq Illumina sequencing platform. *Applied and*  
561 *Environmental Microbiology* 79:5112–20.  
562 Kuzyakov, Y. 2010. Priming effects: Interactions between living and dead organic matter. *Soil*  
563 *Biology and Biochemistry* 42:1363–1371.  
564 Kuzyakov, Y., and E. Blagodatskaya. 2015. Microbial hotspots and hot moments in soil:  
565 Concept & review. *Soil Biology and Biochemistry* 83:184–199.  
566 Lambers, H., C. Mougel, B. Jaillard, and P. Hinsinger. 2009. Plant-microbe-soil interactions in  
567 the rhizosphere: an evolutionary perspective. *Plant and Soil* 321:83–115.  
568 Lange, M., N. Eisenhauer, C. A. Sierra, H. Bessler, C. Engels, R. I. Griffiths, P. G. Mellado-  
569 Vázquez, A. A. Malik, J. Roy, S. Scheu, S. Steinbeiss, B. C. Thomson, S. E. Trumbore,  
570 and G. Gleixner. 2015. Plant diversity increases soil microbial activity and soil carbon  
571 storage. *Nature Communications* 6:6707.

572 Leff, J. W., S. E. Jones, S. M. Prober, A. Barberán, E. T. Borer, J. L. Firn, W. S. Harpole, S. E.  
573 Hobbie, K. S. Hofmockel, J. M. H. Knops, R. L. McCulley, K. L. Pierre, A. C. Risch, E.  
574 W. Seabloom, M. Schütz, C. Steenbock, C. J. Stevens, and N. Fierer. 2015. Consistent  
575 responses of soil microbial communities to elevated nutrient inputs in grasslands across  
576 the globe. *Proceedings of the National Academy of Sciences* 112:10967–10972.

577 Lory, S. 2014. The Family Mycobacteriaceae. Pages 571–575 in E. Rosenberg, E. F. DeLong, S.  
578 Lory, E. Stackebrandt, and F. Thompson, editors. *The Prokaryotes: Actinobacteria*.  
579 Springer Berlin Heidelberg, Berlin, Heidelberg.

580 Meier, I. C., A. C. Finzi, and R. P. Phillips. 2017. Root exudates increase N availability by  
581 stimulating microbial turnover of fast-cycling N pools. *Soil Biology and Biochemistry*  
582 106:119–128.

583 Mevik, B.-H., R. Wehrens, K. H. Liland, and P. Hiemstra. 2019. pls: Partial Least Squares and  
584 Principal Component Regression.

585 Nahlik, A. M., and M. S. Fennessy. 2016. Carbon storage in US wetlands. *Nature*  
586 *Communications* 7:13835.

587 Oksanen, J., F. G. Blanchet, M. Friendly, R. Kindt, P. Legendre, D. McGlenn, P. R. Minchin, R.  
588 B. O’Hara, G. L. Simpson, P. Solymos, M. H. H. Stevens, E. Szoecs, and H. Wagner.  
589 2017. *vegan: Community Ecology Package*.

590 Palma, T. L., M. N. Donaldben, M. C. Costa, and J. D. Carlier. 2018. Putative Role of  
591 *Flavobacterium*, *Dokdonella* and *Methylophilus* Strains in Paracetamol Biodegradation.  
592 *Water, Air, & Soil Pollution* 229:200.

- 593 Parada, A. E., D. M. Needham, and J. A. Fuhrman. 2016. Every base matters: assessing small  
594 subunit rRNA primers for marine microbiomes with mock communities, time series and  
595 global field samples. *Environmental Microbiology* 18:1403–1414.
- 596 Peralta, A. L., and M. M. Wander. 2008. Soil organic matter dynamics under soybean exposed to  
597 elevated [CO<sub>2</sub>]. *Plant and Soil* 303:69–81.
- 598 Riggs, C. E., S. E. Hobbie, E. M. Bach, K. S. Hofmockel, and C. E. Kazanski. 2015. Nitrogen  
599 addition changes grassland soil organic matter decomposition. *Biogeochemistry*  
600 125:203–219.
- 601 Rognes, T., T. Flouri, B. Nichols, C. Quince, and F. Mahé. 2016. VSEARCH: a versatile open  
602 source tool for metagenomics. *PeerJ* 4:e2584.
- 603 Sardans, J., and J. Peñuelas. 2012. The Role of Plants in the Effects of Global Change on  
604 Nutrient Availability and Stoichiometry in the Plant-Soil System. *Plant Physiology*  
605 160:1741–1761.
- 606 Schloss, P. D., S. L. Westcott, T. Ryabin, J. R. Hall, M. Hartmann, E. B. Hollister, R. A.  
607 Lesniewski, B. B. Oakley, D. H. Parks, C. J. Robinson, J. W. Sahl, B. Stres, G. G.  
608 Thallinger, D. J. V. Horn, and C. F. Weber. 2009. Introducing Mothur: open-source,  
609 platform-independent, community-supported software for describing and comparing  
610 microbial communities. *Applied and Environmental Microbiology* 75:7537–7541.
- 611 Sutfin, N. A., E. E. Wohl, and K. A. Dwire. 2016. Banking carbon: a review of organic carbon  
612 storage and physical factors influencing retention in floodplains and riparian ecosystems.  
613 *Earth Surface Processes and Landforms* 41:38–60.

614 Trivedi, P., M. Delgado-Baquerizo, C. Trivedi, H. Hu, I. C. Anderson, T. C. Jeffries, J. Zhou,  
615 and B. K. Singh. 2016. Microbial regulation of the soil carbon cycle: evidence from  
616 gene–enzyme relationships. *The ISME Journal* 10:2593–2604.

617 U.S. Climate Data. 2019. Climate data for Greenville, North Carolina (-77.3984, 35.64) Average  
618 weather Greenville, NC - 27834 - 1981-2010 normals.  
619 <https://www.usclimatedata.com/climate/greenville/north-carolina/united-states/usnc0281>

620 Vitousek, P. M., S. Porder, B. Z. Houlton, and O. A. Chadwick. 2010. Terrestrial phosphorus  
621 limitation: mechanisms, implications, and nitrogen–phosphorus interactions. *Ecological*  
622 *Applications* 20:5–15.

623 Wieder, W. R., C. C. Cleveland, W. K. Smith, and K. Todd-Brown. 2015. Future productivity  
624 and carbon storage limited by terrestrial nutrient availability. *Nature Geoscience* 8:441–  
625 444.

626 Xie, C.-H., and A. Yokota. 2005. *Dyella japonica* gen. nov., sp. nov., a  $\gamma$ -proteobacterium  
627 isolated from soil. *International Journal of Systematic and Evolutionary Microbiology*  
628 55:753–756.

629 Yilmaz, P., L. W. Parfrey, P. Yarza, J. Gerken, E. Pruesse, C. Quast, T. Schweer, J. Peplies, W.  
630 Ludwig, and F. O. Glöckner. 2014. The SILVA and “All-species Living Tree Project  
631 (LTP)” taxonomic frameworks. *Nucleic Acids Research* 42:D643–D648.

632 Young, J. M. 2008. An overview of bacterial nomenclature with special reference to plant  
633 pathogens. *Systematic and Applied Microbiology* 31:405–424.

634  
635  
636

637 **Tables**

638 **Table 1.** Summary of distance-based partial least squares regression (dbpls) representing how  
639 much variation in decomposition rate is explained (%) by each component (Comp) derived from  
640 a tea-associated bacterial community Bray-Curtis distance matrix.

641

	Comp 1	Comp 2	Comp 3	Comp 4	Comp 5	Comp 6
$R^2$	64.96	88.08	94.65	98.12	99.32	99.77
adjusted $R^2$	63.56	87.09	93.96	97.78	99.16	99.70
gvar	31.50	41.62	50.10	56.93	61.21	66.39
crit	2.47	0.91	0.44	0.17	0.07	0.03

642 gvar = total weighted geometric variability; crit = value of criterion defined in method

643

644

645

646

647

648

649

650

651

652

653

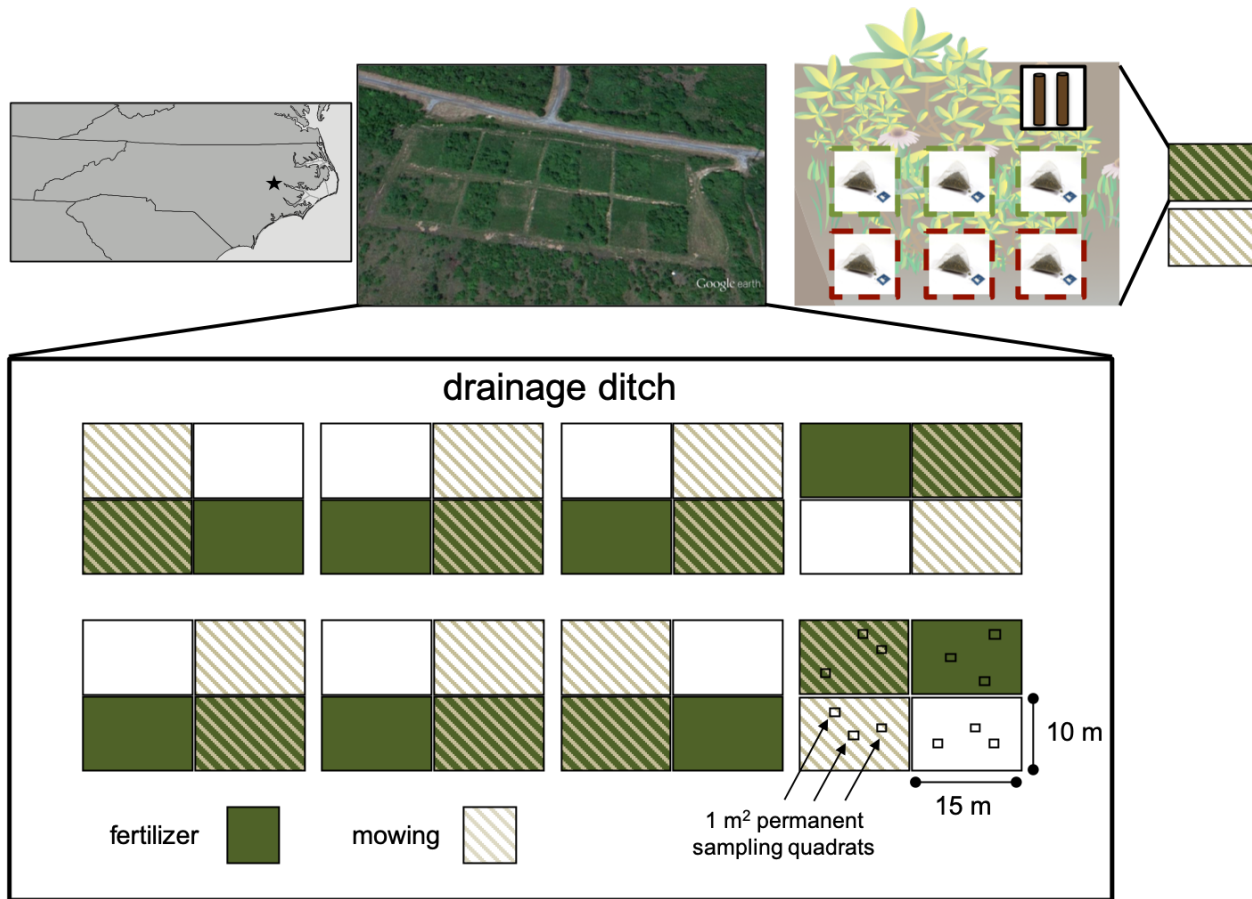
654

655

656

657 **Figures**

658 **Figure 1**

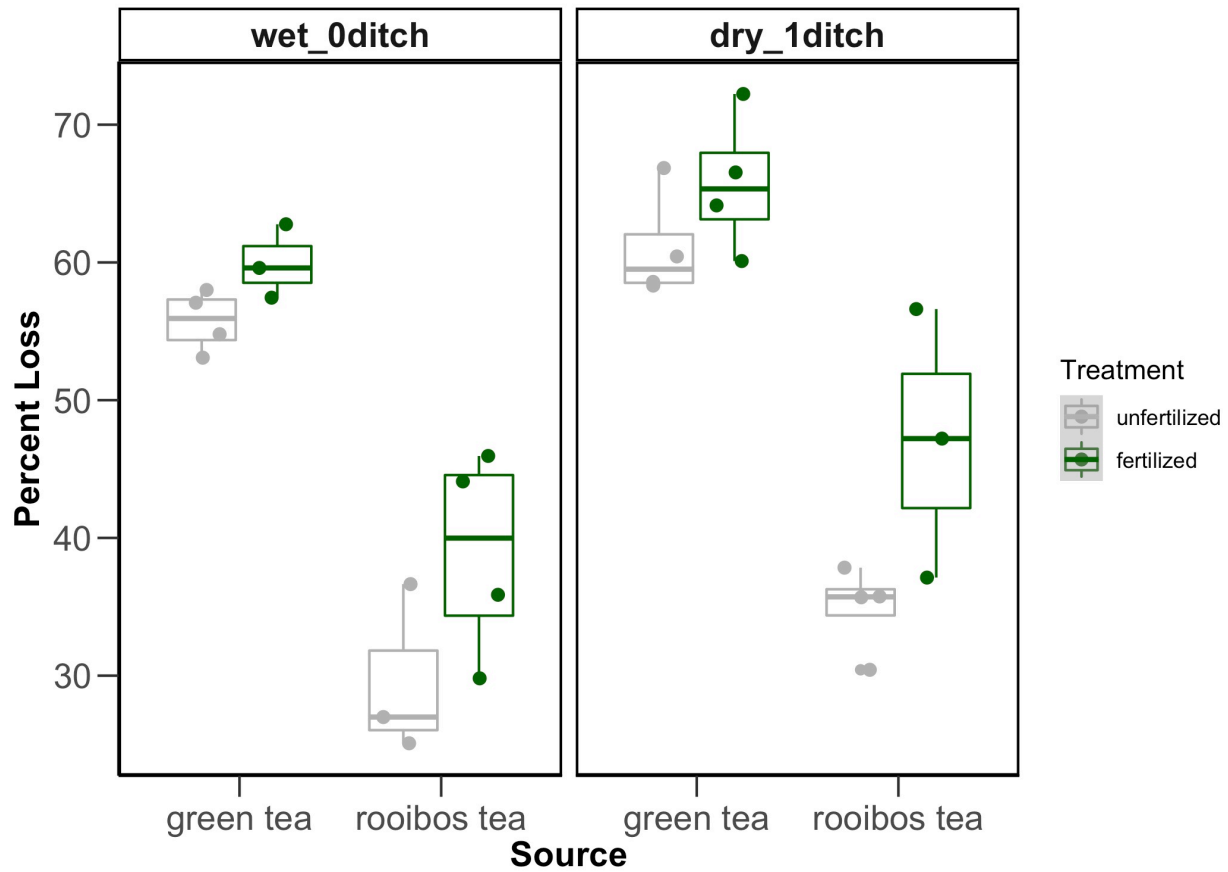


659

660 **Figure 1.** Experimental design of a long-term ecological experiment to test the effects of fertilizer  
661 and disturbance by mowing on plant and microbial communities at East Carolina University's  
662 West Research Campus (WRC), Greenville, NC, USA. The decomposition protocol for this  
663 experiment was adapted from the Tea Bag Index Protocol (Keuskamp et al. 2013)(Keuskamp et  
664 al., 2013) and applied within the eight-replicate fertilized and unfertilized plots of the WRC. In  
665 one quadrat per replicate plot, three bags of Lipton™ green tea and three bags of Lipton™ rooibos  
666 tea were buried and retrieved after 111 days. Bulk soil was sample as a composite sample  
667 representing two soil cores from three permanent quadrats per plot.

668

669 **Figure 2.**



670

671 **Figure 2.** Boxplots representing cumulative mass loss of green (low C:N ratio litter) and rooibos  
672 (high C:N ratio litter) tea in fertilized (green) and unfertilized (gray) plots. Symbols represent  
673 individual data points.

674

675

676

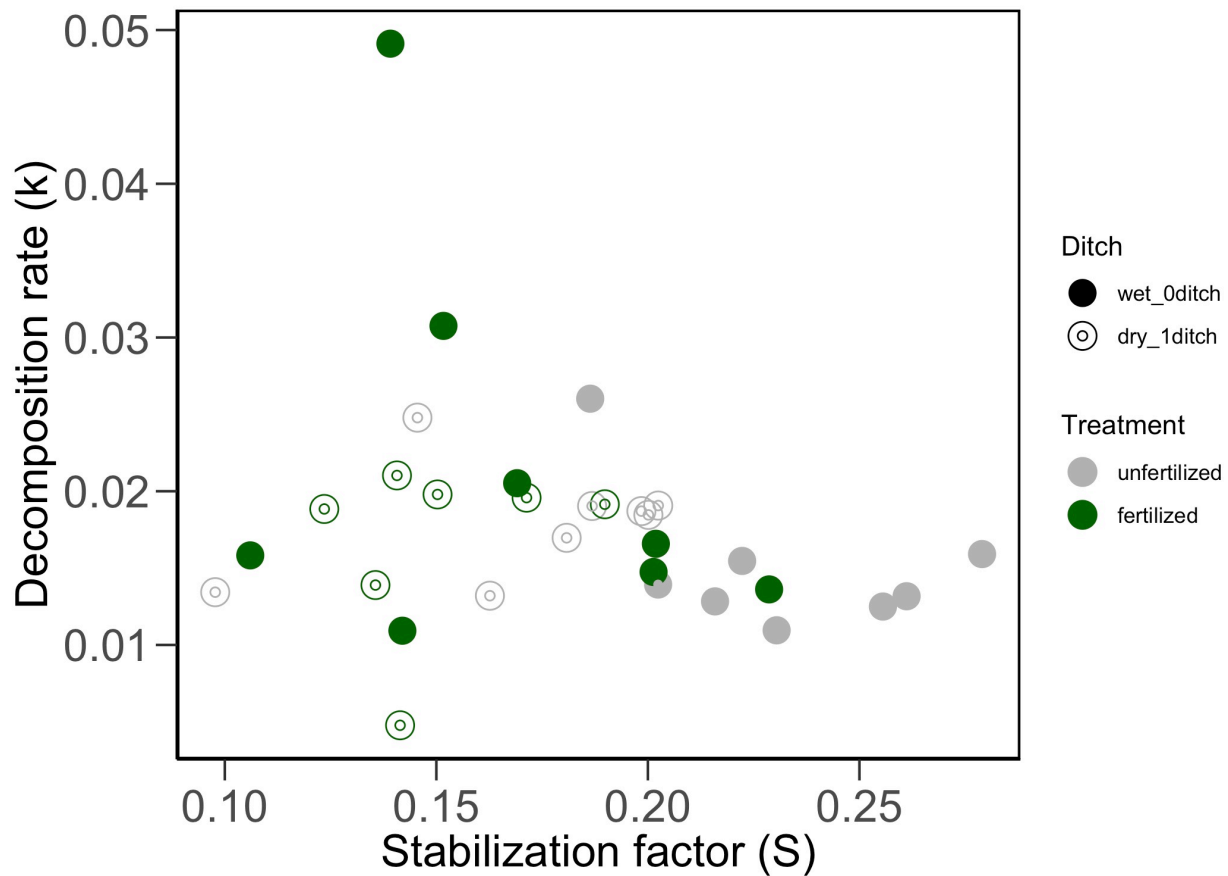
677

678

679

680

681 **Figure 3**



682

683 **Figure 3.** Initial decomposition rate  $k$  and stabilization factor  $S$  for different tea bags within the  
684 long-term fertilization experiment. Tea bags from unfertilized plots are indicated in grey, while  
685 tea bags from fertilized plots are indicated in green. Open symbols represented drier plots that were  
686 closer to the drainage ditch, while closed symbols represented wetter plots that were further from  
687 the ditch.

688

689

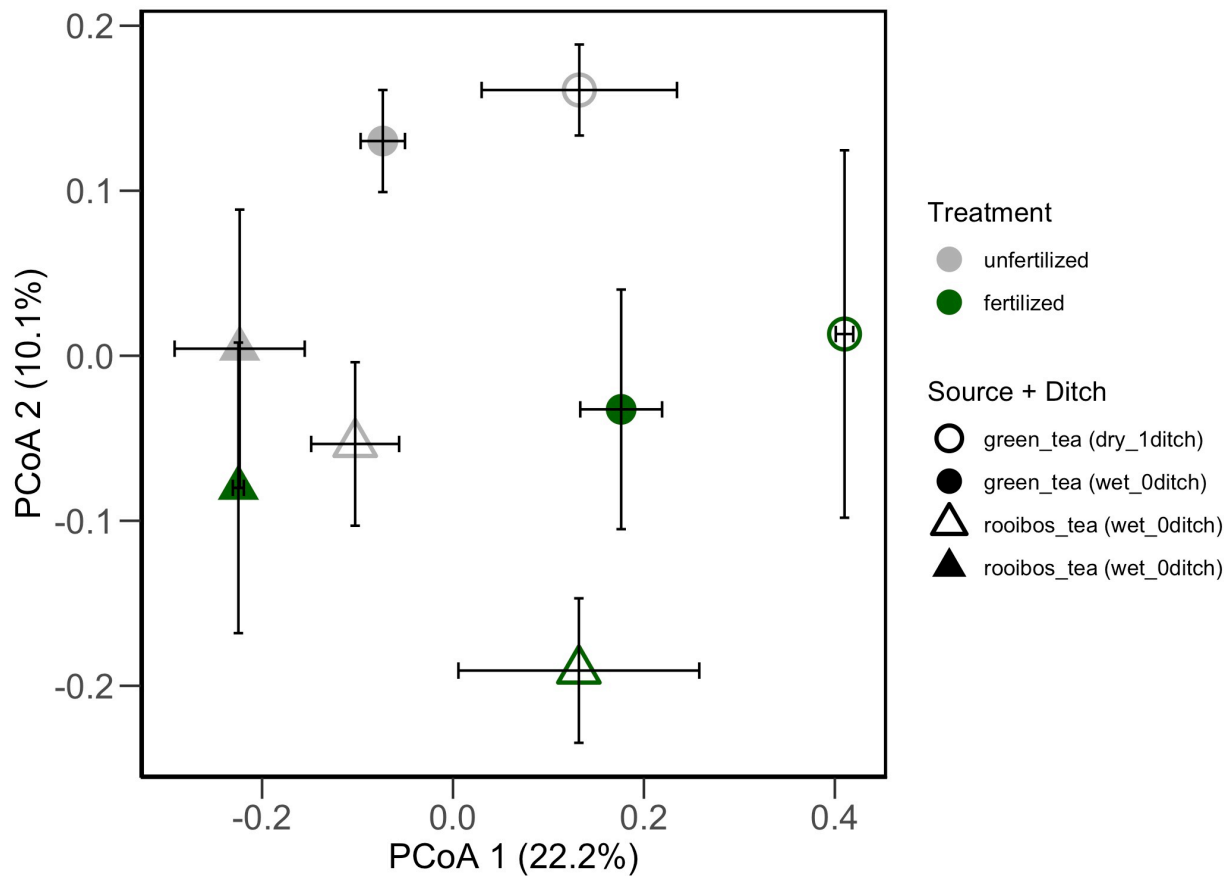
690

691

692



693 **Figure 4**



694

695

696 **Figure 4.** Ordination based on a Principal Coordinates Analysis depicting bacterial community  
697 composition according to tea type. Symbols are colored according to fertilization treatment (gray  
698 = unfertilized, green = fertilized) and tea source (circles = low C:N ratio green tea, triangles = high  
699 C:N ratio rooibos tea) at drier mowed plots situated close to the drainage ditch (open symbols)  
700 compared to wetter mowed plots (closed symbols).

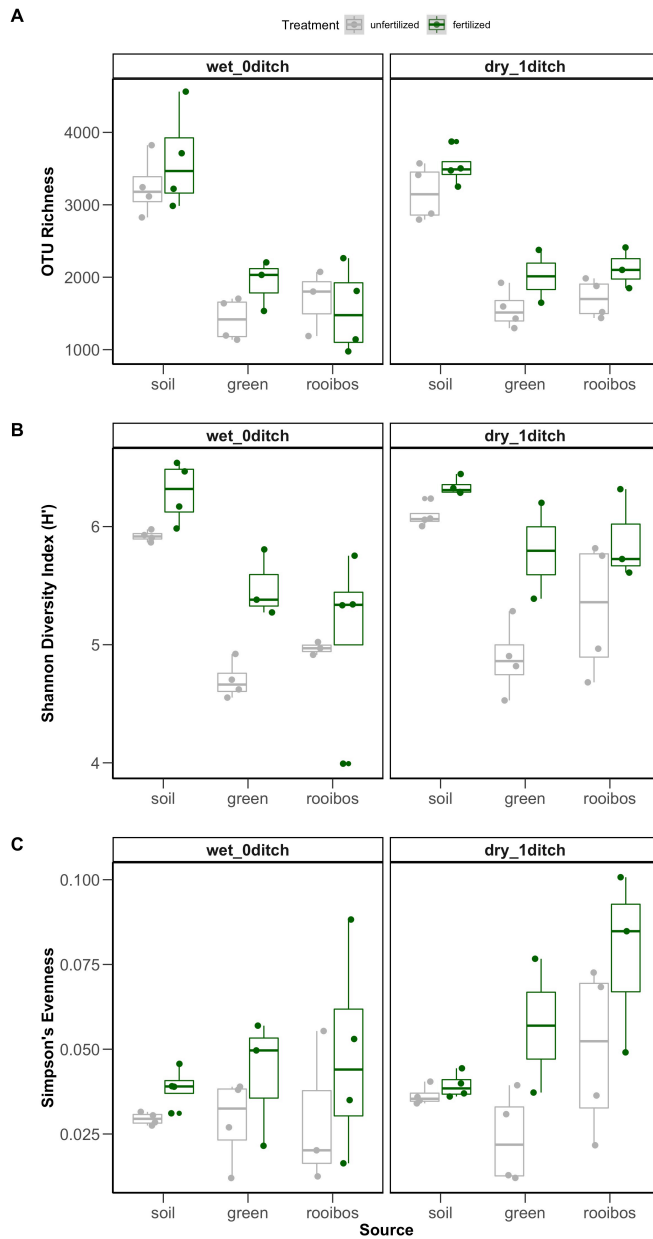
701

702

703

704

705 **Figure 5**



706

707 **Figure 5.** Boxplots depicting of bacterial diversity metrics (OTU richness, Shannon Diversity  
708 Index  $H'$ , and Simpson's Evenness) associated with source (bulk soil, low C:N ratio green tea,  
709 high C:N ratio rooibos tea). Boxplots and symbols are colored according to fertilization treatment  
710 (gray = unfertilized, green = fertilized) at drier mowed plots situated close to the drainage ditch  
711 compared to wetter mowed plots. Symbols represent data points for individual plot samples.